Chemical Engineering Journal 290 (2016) 154–160

Contents lists available at ScienceDirect

Chemical Engineering Journal

journal homepage: www.elsevier.com/locate/cej

Direct delivery of CO_2 into a hydrogen-based membrane biofilm reactor and model development

Siqing Xia [a,*], Xiaoyin Xu [a,b], Chen Zhou [b], Chenhui Wang [a], Lijie Zhou [a], Bruce E. Rittmann [b]

[a] State Key Laboratory of Pollution Control and Resource Reuse, College of Environmental Science and Engineering, Tongji University, 1239 Siping Road, Shanghai 200092, China
[b] Swette Center for Environmental Biotechnology, Biodesign Institute at Arizona State University, 1001 S. McAllister Ave., Tempe, AZ 85287, USA

HIGHLIGHTS

- Direct delivery of CO_2 into fibers improved the hydrogen-based MBfR performance.
- A mathematical model was built up to predict pH and LSI in the system.
- Misdistributions of H_2 and CO_2 caused disparity of biomass communities on different modules.
- Functional bacteria existed on both H_2 and CO_2 modules.

GRAPHICAL ABSTRACT

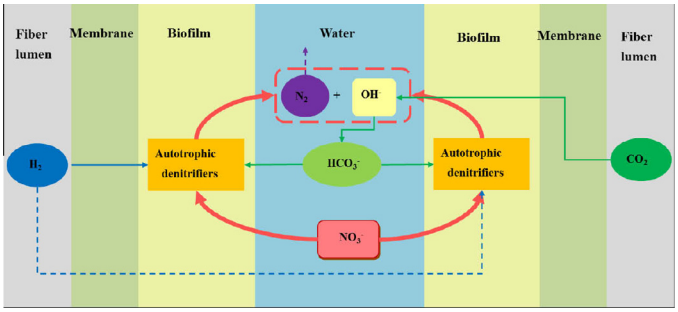

ARTICLE INFO

Article history:
Received 23 September 2015
Received in revised form 9 January 2016
Accepted 11 January 2016
Available online 14 January 2016

Keywords:
MBfR
CO_2
Model
pH control

ABSTRACT

A new hydrogen-based hollow fiber membrane biofilm reactor (MBfR) with double membrane technique was developed in this work and systematic research was conducted. A mathematical model was built up to predict pH and Langelier Saturation Index (LSI) in the hydrogen-based autotrophic denitrification system with minimal error. The model tested with varied CO_2 pressures identified that increasing CO_2 pressure resulted in pH decrease and prevention from precipitation. Long-term performance of the new MBfR was also evaluated. When CO_2 was delivered at 0.05 MPa, 99% nitrate was removed with a constant neutral pH in the reactor. In the long-term experiment, misdistributions of H_2 and CO_2 caused disparity of biomass communities on the H_2 and CO_2 modules, but functional bacteria existed on both modules; this suggested that despite of misdistribution, bubbleless H_2 was still able to be transported by recirculation to the CO_2 module and became available for the bacteria on the module.

1. Introduction

Nitrate is introduced into groundwater from a variety source, such as agricultural activities, poor sewer systems, wastewater, and industrial activities. Nitrate in drinking water is a cause of methemoglobinaemia in infants, and the permissible limit of the World Health Organization (WHO) is 10 mgN/L [1,2]. NO_3^- spurs eutrophication of surface waters, and wastewater standards often are much lower than 10 mgN/L [3].

The H_2-based membrane biofilm reactor (MBfR) was developed to remove nitrate using hydrogen gas as a clean electron-donor substrate for autotrophic denitrifiers [4–7]. One major characteristic of denitrification is base production that can lead to pH increase [7]. Base production in autotrophic denitrification is illustrated in Eqs. (1) and (2) [8],

$$NO_3^- + 1.13H_2 + 0.01H^+ + 0.05CO_2 = 0.99NO_2^- + 0.01C_5H_7O_2N + 1.1H_2O \quad (1)$$

* Corresponding author. Tel.: +86 21 65980440; fax: +86 21 65986313.
E-mail address: siqingxia@gmail.com (S. Xia).

http://dx.doi.org/10.1016/j.cej.2016.01.021
1385-8947/

$$0.99NO_2^- + 1.76H_2 + 0.99H^+ + 0.12CO_2 = 0.483N_2 + 0.0242C_5H_7O_2N + 2.17H_2O \quad (2)$$

in which hydrogen gas (H_2) is the electron donor and biomass synthesis is indicated by $C_5H_7O_2N$. Nitrite reduction is the predominant source of alkalinity, consuming 1 H^+ equivalent per N equivalent of NO_2^-. Denitrification also consumes some inorganic carbon for biomass synthesis, although its impact is small compared to the generation of base.

One risk from proton consumption is high-pH inhibition [9]. For example, Lee and Rittmann (2003) reported that the optimal pH for autotrophic denitrification is in the range 7.7–8.6, and a significant decrease in nitrate removal rate and a dramatic increase in nitrite accumulation occur with pH over 8.6. Another risk of high pH is the precipitation of hardness cations with common basic anions. Common mineral precipitates in biological denitrification processes include calcium carbonate ($CaCO_3$), calcium hydrogen phosphate ($CaHPO_4$), calcium dihydrogen phosphate ($Ca(H_2PO_4)_2$), hydroxyapatite ($Ca_5(PO_4)_3OH$), and β-tricalcium phosphate ($Ca_3(PO_4)_2$) [10]. Precipitation of mineral solids on the membrane can lead to long-term loss of gas permeability and to embrittlement of the membrane in an MBfR [4,7]. Consequently, pH control is necessary for autotrophic denitrification.

Phosphate buffer ($KH_2PO_4 + Na_2HPO_4$) has been used extensively as a pH buffer in bench-scale MBfR studies [11–18]. However, phosphate also can lead to surface-water eutrophication [19,20] when the effluent is discharged to a surface water, and it also has been reported to stimulate microbial growth in distribution systems in special circumstances [21]. According to stoichiometry, when the influent nitrate is 10 mg N/L, the concentration of phosphate buffer must be above 100 mg P/L buffer ($Na_2HPO_4 + KH_2PO_4$) to keep the effluent pH below 8.0.

A better alternative for pH control is carbon dioxide gas (CO_2), which also is the inorganic carbon source for H_2-based autotrophic denitrification and is not harmful to humans or the aquatic environment. Tang et al. (2011) sparged CO_2 directly into pilot-scale MBfRs and successfully maintained the effluent pH below 8.0. Commercial-scale MBfRs use CO_2 sparging to control pH. A pH probe actuates CO_2 sparging whenever the pH inside the MBfR exceeds a set point, such as 7.5–8.0.

While effective for pH control, CO_2 sparging can lead to CO_2 loss in the off-gas, which wastes CO_2 and increases operating costs. Here we apply a novel double-membrane technique to overcome the drawbacks of CO_2 sparging. CO_2 is delivered to hollow-fibers simultaneously with H_2 so that it diffuses into water in the same "bubbleless" way as H_2 [22]. This approach offers a means to eliminate CO_2 loss by off-gasing. We investigated the performance of an MBfR when using different CO_2 pressures and developed a model to predict the effluent pH and precipitation risk.

2. Model development

2.1. Model overview

Three major factors affect the pH in our MBfR system. The first factor is the alkalinity present in feed water. For natural water, the carbonate system dominates the alkalinity due to the common occurrence and dissolution of carbonate minerals and the presence of CO_2 in the atmosphere [10]. The second factor is the CO_2 addition (via membrane diffusion). CO_2 is the acid form of inorganic carbon, and its addition lowers the pH while increasing the total inorganic carbon. The third factor is the denitrification and oxygen respiration processes in our system. The base production and consumption of CO_2 in denitrification were illustrated in Eqs. (1) and (2). Dissolved oxygen almost always is present in water to be treated by denitrification. While respiration of O_2 does not consume significant protons, oxygen respiration can affect the pH by CO_2 consumption in an autotrophic system (Eq. (3)) [23]:

$$O_2 + 2.39H_2 + 0.0282NO_3^- + 0.141CO_2 + 0.0282H^+ = 0.0282C_5H_7O_2N + 2.31H_2O \quad (3)$$

When coupled with an alkalinity mass balance (via the proton condition) in the influent and effluent, the factors mentioned above can be used to create a model to predict the effluent pH and alkalinity, from which the Langelier Saturation Index (LSI) can be computed to give an indication of the precipitation potential for $CaCO_3$, the most common mineral precipitate.

2.2. Assumptions and simplifications

The model makes the following simplifying assumptions, which are based on Tang et al. (2011):

(1) The pH inside the biofilm does not differ greatly from that in the bulk liquid. Therefore, the conditions in the bulk liquid can be used to assess alkalinity, pH, and LSI based on denitrification reactions occurring in the biofilm.
(2) Inorganic-carbon species are the only buffers, since phosphate concentrations normally are low [24].
(3) Calcium carbonate ($CaCO_3$) is the only precipitate. Calcium phosphate species are neglected, since the phosphate concentration typically is low. $Mg(OH)_2$ also is neglected, because it is super-saturated only at pH values that are too high to be relevant for biological treatment [10].
(4) The reactor is a closed system, which means that CO_2 does not exchange between the reactor and the atmosphere.
(5) Activity coefficients are ignored, since most waters for denitrification have a low salinity.

2.3. Theoretical approach

The alkalinity in the influent and effluent of the reactor is tabulated by coupling the proton condition, the total concentration of inorganic carbonate species (C_T), and the hydrogen-ion concentration (Eq. (4)).

$$\begin{aligned}[Alk] &= 2[CO_3^{2-}] + [HCO_3^-] + [OH^-] - [H^+] \\ &= 2[C_T]\frac{1}{1+[H^+]/K_2+[H^+]^2/K_1K_2} \\ &+ [C_T]\frac{1}{1+[H^+]/K_1+K_2/[H^+]} + \frac{10^{-14}}{[H^+]} - [H^+]\end{aligned} \quad (4)$$

in which K_1, K_2 = acid/base equilibrium constants for H_2CO_3 and HCO_3^- ($K_1 = 10^{-6.3}$, $K_2 = 10^{-10.3}$ at 2 °C); and C_T = total concentration of inorganic carbon species in the influent and effluent (mole/L).

Eq. (4) can be used to obtain $C_{T,in}$, since $[Alk]_{in}$ and $[H^+]_{in}$ can be measured. Then $C_{T,out}$ can be solved by calculating the change of total concentration of inorganic carbon species due to denitrification (Eqs. (1) and (2)), oxygen respiration (Eq. (3)), precipitation, and external CO_2 addition. $[NO_3^-]_{in}$, $[NO_3^-]_{out}$, $[Ca^{2+}]_{in}$, $[Ca^{2+}]_{out}$, $[O_2]_{in}$, and $[O_2]_{out}$ are experimentally measured model inputs and the concentration of the external CO_2 addition $[CO_2]$ can be calculated via CO_2 permeability, which can be obtained from Siqing et. al. (2015) [25].

$[Alk]_{out}$ can be solved by calculating the change of alkalinity due to denitrification (Eqs. (1) and (2)), oxygen respiration (Eq. (3)), precipitation, and external acid addition. $[NO_3^-]_{in}$, $[NO_3^-]_{out}$, $[Ca^{2+}]_{in}$, $[Ca^{2+}]_{out}$, $[O_2]_{in}$, and $[O_2]_{out}$ are experimentally measured model inputs and the external acid addition is not involved in our research.

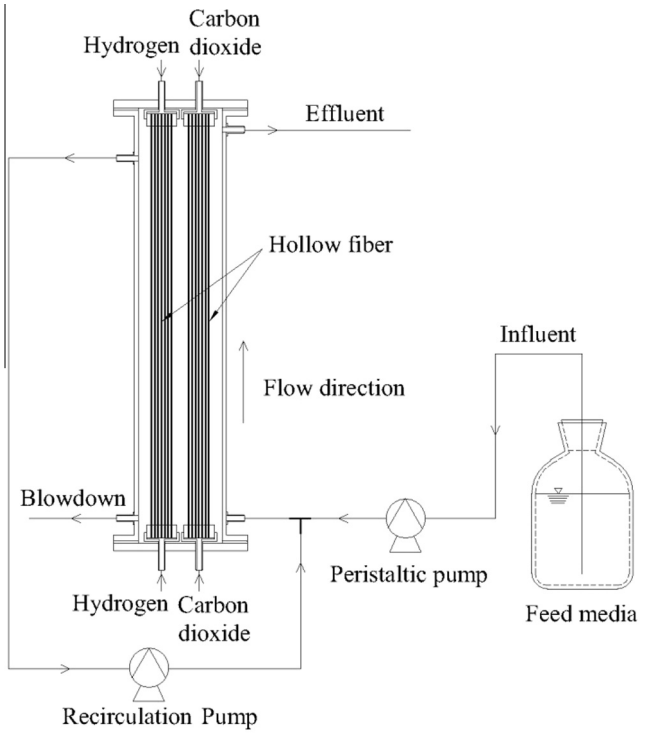

Fig. 1. Schematic of the new type H_2-based membrane biofilm reactor (MBfR).

As long as we solved $C_{T,out}$ and $[Alk]_{out}$, the effluent pH ($[H^+]_{out}$) can be obtained by solving Eq. (4). After that, LSI can be computed using Eq. (5).

$$LSI = pH - \left(pK_2 - pK_{so} + p\left[Ca^{2+}\right]_{out} + p\left[HCO_3^-\right]_{out}\right) \quad (5)$$

where K_{so} = solubility product for $CaCO_{3(s)}$ ($10^{-8.3}$ at 25 °C).

3. Experimental methods

3.1. Experimental setup

Fig. 1 illustrates the bench-scale MBfR, which was modified from a previous one [26,27]. The total volume was enlarged from 600 mL to 3.46 L, and two identical membrane modules were inserted into it, providing a membrane surface area of 2750 cm^2 for each module. The gas-transfer fibers were made of polyvinylidene difluoride (PVDF) with pore size of 0.1 μm (Litree Company, Suzhou, China). Pure H_2 or CO_2 was supplied into each module via a metering valve and diffused through the walls of the PVDF membranes. The MBfR was operated in a continuous mode with an influent flow rate of 2 mL/min and a recirculation rate of 150 mL/min, which gave completely mixed conditions inside the MBfR.

Table 2
Comparison of the measured and model-predicted pH and LSI for autotrophic denitrification.

CO_2 pressure:		0.03 MPa	0.04 MPa	0.05 MPa	0.06 MPa
pH	Measured	7.61 ± 0.14	7.48 ± 0.08	7.35 ± 0.03	7.13 ± 0.02
	Model-predicted	7.67	7.46	7.44	7.03
	Difference (%)	0.78	−0.26	1.22	−1.40
LSI	Measured	0.29	0.17	0.05	−0.27
	Model-predicted	0.35	0.15	0.13	−0.27
	Difference	0.06	−0.02	0.08	0

The groundwater was collected from a 15-m deep well (Shanghai Maling Aquarius Co., Ltd.) routinely. The concentrations of nitrate and sulfate were minimal, but concentrations of Ca^{2+} and Mg^{2+} were high: 55 (±5) mg/L and 25 (±5) mg/L, respectively. Nitrate (10 mgN/L) was added to the groundwater before feeding it to the MBfR.

The inoculum was taken from an existing MBfR in which autohydrogenotrophic denitrifying bacteria had been acclimated for several months. Start-up of the MBfR began when H_2 and CO_2 were supplied to the membrane modules at a pressure of 0.02 MPa, and the liquid influent flow rate was set at 0.2 mL/min. The reactor was operated intermittently for 2 days by feeding the amended groundwater for 12 h per day to establish a biofilm on the membrane surface. After start up, the H_2 pressure was increased to 0.06 MPa, and the influent flow rate was set at 2 mL/min. The CO_2 pressure was adjusted as needed to keep the effluent pH between 7.0 and 7.5. When the reactor reached steady state for nitrate removal, the CO_2 pressure was systematically varied at 0.03, 0.04, 0.05, and 0.06 MPa to investigate how the CO_2 pressure affected effluent pH, nitrate reduction, and calcium precipitation. For each CO_2 pressure, the change of system conditions lasted for 7 d before the effluent was sampled. With a hydraulic retention time (HRT) of 28.8 h in the MBfR, 7 d (more than 5 HRTs) was long enough for the system to reach a pseudo steady-state, which is defined as a condition in which the liquid concentration reached a stable state, while the biofilm accumulation and the biomass were not changed significantly from the actual steady state. Long-term experiments (72 days) also were carried out with CO_2 pressures of 0.03 MPa and 0.05 MPa to assess the MBfR performance and stability under optimal and extreme CO_2 pressures.

3.2. Sampling and analyses

All fluid samples were filtered through a 0.22-μm polyether sulfone membrane filter (Anpel Company, Shanghai, China). NO_3^-—N and NO_2^-—N were analyzed by ion chromatography (ICS-1000, Dionex, USA) using an AS-20 column, an AG-20 guard column, and a 150-mg/L injection loop [27]. Ca(II) concentration was measured by inductively coupled plasma (ICP-OES) (DV2100, PE, USA). pH was measured with a pHS-29A meter (HACH, USA). Calcified membrane fibers obtained in the long-term experiments with

Table 1
Experimentally measured model inputs for the autotrophic denitrification.

CO_2 pressure:	0.03 MPa		0.04 MPa		0.05 MPa		0.06 MPa	
	Influent	Effluent	Influent	Effluent	Influent	Effluent	Influent	Effluent
DO (mg/L)	0.2 ± 0.2	0	0.2 ± 0.1	0	0	0	0.2 ± 0.1	0
NO_3^- (mg/L)	10.1 ± 0.1	0.02 ± 0.02	10.2 ± 0.4	0.04 ± 0.01	10.4 ± 0.2	0.1 ± 0.01	10.6 ± 0.5	0.7 ± 0.04
NO_2^- (mg/L)	0	0	0	0	0	0	0	0
Ca^{2+} (mg/L)	60.2 ± 0.7	57.8 ± 0.2	58.0 ± 0.8	57.4 ± 0.3	61.2 ± 0.1	61.2 ± 0.1	60.5 ± 0.4	60.6 ± 0.4
PO_4^{3-} (mg/L)	1.5	<0.01	1.8	<0.01	2.3	<0.01	0.8	<0.01
pH	7.25 ± 0.01	7.61 ± 0.14	7.32 ± 0.03	7.48 ± 0.08	7.34 ± 0.1	7.35 ± 0.03	7.15 ± 0.07	7.13 ± 0.02
Alkalinity [a] (mg/L as $CaCO_3$)	301 ± 1	329.4	301 ± 1	334.8	301 ± 1	337.6	301 ± 1	337.3

[a] Influent alkalinity was experimentally measured and effluent alkalinity was calculated.

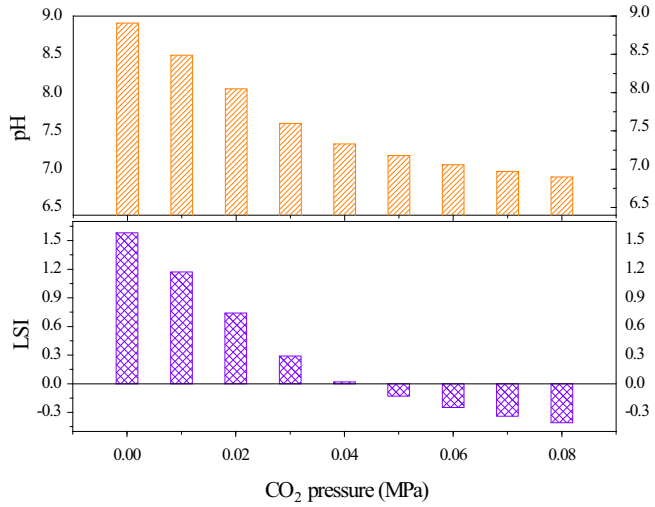

Fig. 2. Model-predicted pH, alkalinity, and LSI under varied CO_2 pressures in the autotrophic system. (The scenario was assumed based on the experiment results: nitrate is 10 mg/L in influent and 100% removed. Influent pH and alkalinity is 7.2 and 300 mg/L (as $CaCO_3$), respectively.)

0.03 MPa CO_2 were rinsed three times with DI water, air-dried [28], and analyzed with a scanning electron microscope (SEM) equipped with an energy dispersive spectrometer (EDS) (XL30, PHILIPS, NL).

3.3. 16S rRNA clone library construction

Biomass samples were obtained from the hydrogen-module (named as "Hydrogen"), and carbon dioxide-module (named as "Carbon dioxide") in the long-term experiments with the higher CO_2 pressure (day 72 from the startup stage). The attached biofilm was removed using a vortex mixer and borosilicate glass balls and suspended in PBS buffer (Na_2HPO_4, KH_2PO_4, NaCl, and KCl) for three times [29,30]. For DNA extractions, the samples were put into bead tubes (MP Biomedical, LLC, France), and genomic DNA was extracted following the manufacturer's protocol. We amplified the extracted DNA with the bacterial universal primers 27f [5′-AGAGTTTGATCCTGGCTCAG-3′] and 1492r [5′-GGTTACCTTGTTACGACTT-3′] and purified it with a QIAquick PCR purification kit (QIAGEN) [31]. For 16S rDNA gene cloning, we inserted the purified PCR amplicons into a cloning vector. The individual PCR amplicons in each vector were cloned via growth of the host cells on an ampicillin-supplemented LB medium. When the vectors containing PCR products were isolated, we randomly selected 120 clones from each sample for sequencing (BGI, Shanghai, China); 102 clones for Hydrogen and 100 clones for carbon dioxide gave successful results. A phylogenetic tree was constructed using the neighbor-joining algorithm in MEGA5 software. The 16S rRNA gene sequences from this study have been deposited in National Institutes of Health (NIH) genetic sequence database (GenBank) under accession numbers KM016243–KM016330.

4. Results and discussion

4.1. The MBfR performance under different CO_2 pressure

The effects of CO_2 pressure on denitrification, calcium precipitation, and pH are investigated. We sampled the MBfR every day to monitor its performance (Fig. S1). For each CO_2 pressure, liquid concentrations and pH reached a pseudo steady-state around day 4. Thus, the last three samples (samples on day 5, day 6. and day

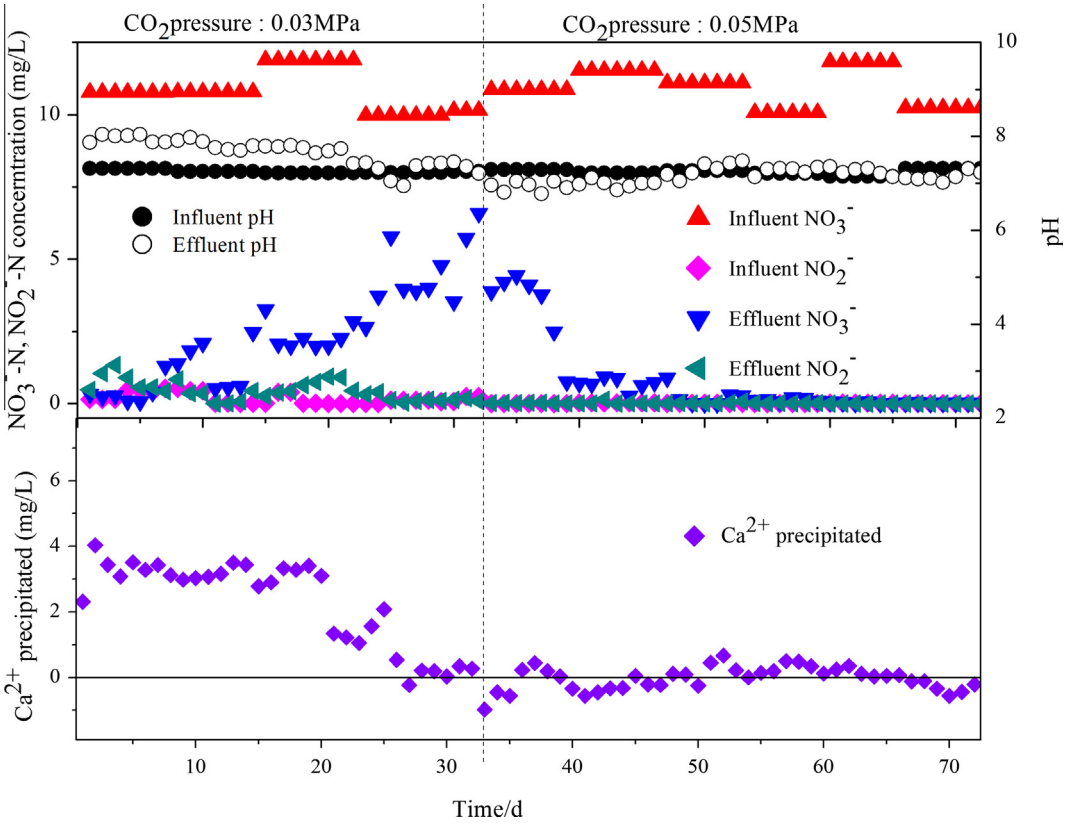

Fig. 3. Influent and effluent concentrations of NO_3^- and NO_2^- (upper left *Y* axis in mg N/L), pH (upper right *Y* axis), and Ca^{2+} precipitation (lower left *Y* axis in mg/L) in the long-term experiment with two different CO_2 pressures (day 0–33: 0.03 MPa, day 34–73: 0.06 MPa).

7) for each stage were used to calculate the experimentally measured model inputs (Table 1).

With CO_2 pressure increased from 0.03 MPa to 0.06 MPa, the effluent pH decreased from 7.61 to 7.13 step by step. On stage 4, when the CO_2 pressure was increased to 0.06 MPa, the effluent nitrate concentration had a tiny increase with effluent pH approaching 7. One major reason is slightly alkaline conditions are preferred by autohydrogenotrophic denitrifiers. Fig. S1 also reflects the precipitation of Ca^{2+} in the reactor: Ca^{2+} in effluent significantly lower than that in influent under 0.03 MPa CO_2 pressure. Increasing CO_2 pressure can reduce Ca^{2+} precipitation. When CO_2 pressure increased to 0.05 MPa, the Ca^{2+} precipitation was not detected. In sum, CO_2 pressure increase results in pH reduce and refrain from precipitation only with slightly low pH inhibition for the bioreduction.

4.2. Model evaluation and necessity of pH control

The model is evaluated based on the inputs listed in Table 1. Table 2 presents a comparison of the measured effluent pH and LSI with the model-predict values. The model outputs of the pH have an error of less than 2% for all cases, and the LSI deviates by less than 0.08 LSI units.

In order to highlight the effect of CO_2 pressure and the necessity to control the pH, Fig. 2 presents the model simulations of the effluent pH and LSI under different CO_2 pressures. A scenario similar with the experiment was set up: $[NO_3^-]_{in}$ is 10 mg/L and 100% removed. Influent pH and alkalinity is 7.2 and 300 mg/L (as $CaCO_3$), respectively. We also assumed no precipitation ($[Ca^{2+}]_{out} = [Ca^{2+}]_{in}$) when solving Eqs. (4) and (5). The latter is a simplification that yields the maximum effluent precipitation risk displayed as the LSI. The scenario without CO_2 addition (CO_2 pressure = 0 MPa) was predicted to have high pH (8.2) and LSI (0.89). In practice, an LSI above 0.5 leads to noticeably increased scaling [32]. So, LSI = 0 was used here in order to incorporate a safety factor. As the CO_2 pressure increasing, the effluent pH and LSI decreased, as well as the precipitation risk. According to the model, optimal CO_2 pressure is 0.05 MPa for the settled scenario, when LSI was just below 0 and precipitation risk was eliminated. Keep increasing CO_2 pressure lead to lower pH, which was not preferred by autohydrogenotrophic denitrifiers, and CO_2 oversupply is a waste of resource.

In sum, CO_2 pressure control is with significant necessity. The mathematical model can be used to estimate the amount of CO_2 added to the reactor or the pH set point to prevent the pH from exceeding the optimal range for denitrification and to prevent precipitation from occurring. Optimal CO_2 pressure can be calculated according to the model before a project carried out.

4.3. Long-term performance under low and optimal CO_2 pressures

As elucidated in Fig. 3, the performance of MBfR was investigated under low CO_2 pressure (0.03 MPa) and optimal CO_2 pressure (0.05 MPa) respectively. In the first few days of the low CO_2 pressure condition, a small amount of nitrite was detected in the effluent and then decreased; identifying nitrate had degraded to nitrite and nitrogen gas step by step. On day 7, 99% nitrate was removed, while the effluent pH was approaching 8 and Ca^{2+} precipitation was detected, indicating that CO_2 was insufficient to neutralize the base produced during denitrification and keep the pH neutral. On day 8, the effluent nitrate bumped up to 1.29 mg/L and kept increasing. On day 32, the effluent nitrate concentration increased to 6.58 mg/L, and the denitrification rate decreased to 34%. The observed decrease tendency of the effluent pH was due to the low denitrification rate. By the end of the low CO_2 pressure condition, the fibers were covered by visible precipitate, which leads to calcified membrane and inhibit the denitrification.

After the modules were rinsed and re-inoculated, we started experiment with optimal CO_2 pressure (0.05 MPa) on day 33. The effluent nitrate kept decreasing once the high CO_2 pressure condition started (Fig. 3). Steady state reduction of nitrate was evident on day 48, with the average removal of nitrate up to 99%. In addition, the effluent pH maintained neutral and calcium precipitation was not observed in this condition, indicating that an appropriate CO_2 pressure inhibited the risk of severe pH.

4.4. Solid characterization of biofilm samples

The SEM samples were obtained after the MBfR was running for 32 days under low CO_2 pressure condition (0.03 MPa). By then, the fibers were covered by visible precipitate, especially the hydrogen module. Fig. 4 showed the surface morphologies with two different enlargement factors of the calcified fibers. The precipitate represents typical inorganic crystal. EDS analysis of the crystal area in the region V_a = 15.0 kV is employed to determine the component of the inorganic crystal. The raw data of EDS spectra were shown in Fig. S2. After automatic calculation, the results showed that calcium, carbon, and oxygen are the main elements, with atom percentage at 19.96%, 13.88% and 65.97%, respectively, speculating that the precipitate could be $CaCO_3$.

4.5. Phylogenetic analysis

Phylogenetic analysis is conducted to investigate the community disparity between the H_2 and the CO_2 module, and phylogenetic trees are presented in Figs. S3 and S4. The clones for each

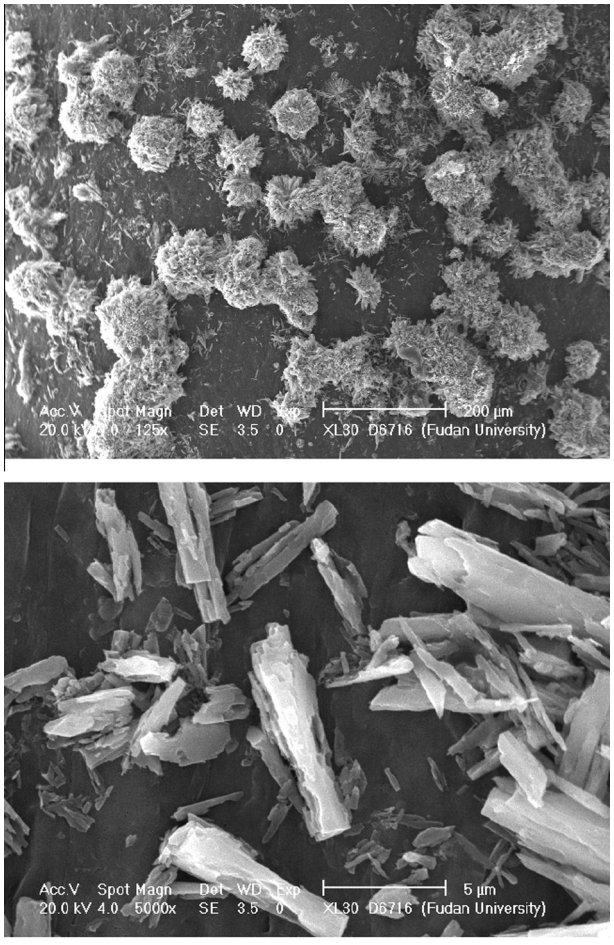

Fig. 4. SEM analysis of the precipitate from the cacified fiber in the long-term experiment with low CO_2 pressure (0.03 MPa).

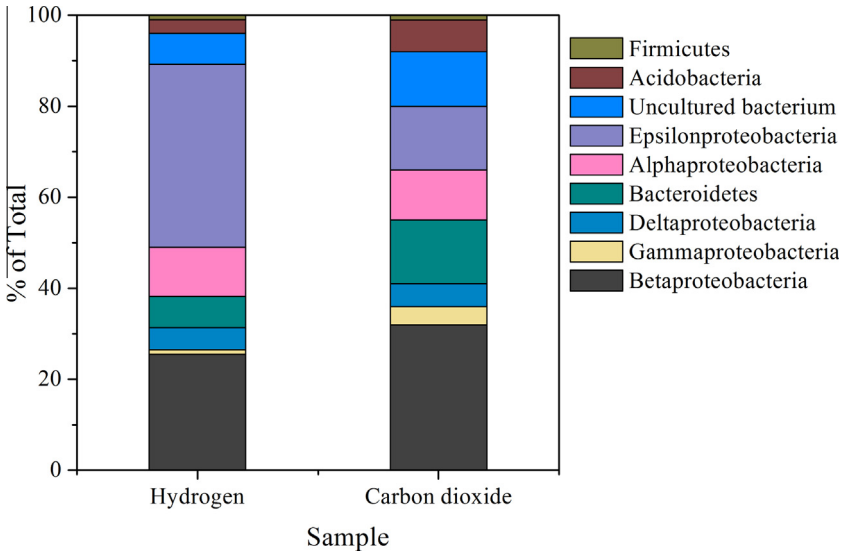

Fig. 5. Microbial community compositions of the H_2 and CO_2 module on day 72 in long-term experiment.

sample are grouped into 43 OTUs (H_2 module) and 45 OTUs (CO_2 module), on the basis of more than 97% sequence similarity within an OTU. Fig. 5 illustrates the microbial community compositions. In the Hydrogen community, *ε-proteobacteria* (40.2%), *β-proteobacteria* (25.5%), *α-proteobacteria* (10.8%) and *Bacteroidetes* (6.86%) were identified as dominant species. In the carbon dioxide community, *β-proteobacteria* (32.0%), *ε-proteobacteria* (14.0%), *Bacteroidetes* (14.0%), and *α-proteobacteria* (11.0%) were major populations. The distinctions between the community compositions are due to the H_2 and CO_2 usage disparity. H_2 and CO_2 diffuse through the hollow-fiber wall, dissolved in the water and partially utilize by the biofilm. During this process, one major disparity is the difference of permeability for CO_2 and H_2. Another issue is that CO_2 can be easily transferred in the water due to its relatively high solubility while H_2 can be misdistributed from H_2 module to CO_2 module due to its low solubility.

Despite of the distinction, it's noteworthy that a previously kwon functional denitrifier, *Rhodocyclus*, was observed on both modules. *Rhodocyclus* was reported has the capacity to grow chemoautotrophically based on H_2 oxidation with either oxygen or nitrate as the electron acceptor. This suggested that despite of misdistribution, bubbleless H_2 was still able to be transported by recirculation to the CO_2 module and became available for the bacteria on that module. However, since bacteria on CO_2 modules can hardly use H_2 due to its low solubility, the enrichment of functional bacteria on CO_2 module is more difficult than that on H_2 module. Increasing the utilization of H_2 on CO_2 module can increase the utilization of the membrane surface and then improve our MBfR's efficiency.

5. Conclusions

This work presents a new hydrogen-based MBfR with double membrane technique to deliver H_2 as the electron donor and CO_2 as the carbon source and exclusive pH adjuster simultaneously. A mathematical model was built up to predict pH and LSI in the system. Distinctions of community compositions exist between H_2 and CO_2 modules while functional bacterium was observed on both modules, suggested that despite of misdistribution, bubbleless H_2 was still able to be transported by recirculation to the CO_2 module and became available for the bacteria on the module.

Acknowledgements

This work is supported by National Natural Science Foundation of China (51378368).

Appendix A. Supplementary data

Supplementary data associated with this article can be found, in the online version, at http://dx.doi.org/10.1016/j.cej.2016.01.021.

References

[1] W.J. Showers, B. Genna, T. McDade, R. Bolich, J.C. Fountain, Nitrate contamination in groundwater on an urbanized dairy farm, Environ. Sci. Technol. 42 (2008) 4683–4688.
[2] R. Yang, W. Liu, Nitrate contamination of groundwater in an agroecosystem in Zhangye Oasis, Northwest China, Environ. Earth Sci. 61 (2010) 123–129.
[3] D.C. Herman, W.T. Frankenberger, Bacterial reduction of perchlorate and nitrate in water, J. Environ. Qual. 28 (1999) 1018–1024.
[4] M.C. Ziv-El, B.E. Rittmann, Systematic evaluation of nitrate and perchlorate bioreduction kinetics in groundwater using a hydrogen-based membrane biofilm reactor, Water Res. 43 (2009) 173–181.
[5] S. Xia, Y. Zhang, F. Zhong, A continuous stirred hydrogen-based polyvinyl chloride membrane biofilm reactor for the treatment of nitrate contaminated drinking water, Bioresour. Technol. 100 (2009) 6223–6228.
[6] S. Xia, F. Zhong, Y. Zhang, H. Li, X. Yang, Bio-reduction of nitrate from groundwater using a hydrogen-based membrane biofilm reactor, J. Environ. Sci. 22 (2010) 257–262.
[7] K.-C. Lee, B.E. Rittmann, Effects of pH and precipitation on autohydrogenotrophic denitrification using the hollow-fiber membrane-biofilm reactor, Water Res. 37 (2003) 1551–1556.
[8] B.E. Rittmann, P.L. McCarty, Environmental Biotechnology: Principles and Applications, Tata McGraw-Hill Education, 2012.
[9] J.H. Hwang, N. Cicek, J.A. Oleszkiewicz, Inorganic precipitation during autotrophic denitrification under various operating conditions, Environ. Technol. 30 (2009) 1475–1485.
[10] V.L. Snoeyink, D. Jenkins, Water Chemistry, John Wiley, 1980.
[11] H.P. Zhao, S. Van Ginkel, Y. Tang, D.W. Kang, B. Rittmann, R. Krajmalnik-Brown, Interactions between perchlorate and nitrate reductions in the biofilm of a hydrogen-based membrane biofilm reactor, Environ. Sci. Technol. 45 (2011) 10155–10162.
[12] A. Ontiveros-Valencia, M. Ziv-El, H.P. Zhao, L. Feng, B.E. Rittmann, R. Krajmalnik-Brown, Interactions between nitrate-reducing and sulfate-reducing bacteria coexisting in a hydrogen-fed biofilm, Environ. Sci. Technol. 46 (2012) 11289–11298.
[13] A. Ontiveros-Valencia, Y. Tang, R. Krajmalnik-Brown, B.E. Rittmann, Managing the interactions between sulfate- and perchlorate-reducing bacteria when using hydrogen-fed biofilms to treat a groundwater with a high perchlorate concentration, Water Res. 55 (2014) 215–224.

[14] A. Ontiveros-Valencia, Y. Tang, R. Krajmalnik-Brown, B.E. Rittmann, Perchlorate reduction from a highly contaminated groundwater in the presence of sulfate-reducing bacteria in a hydrogen-fed biofilm, Biotechnol. Bioeng. 110 (2013) 3139–3147.
[15] R. Nerenberg, Y. Kawagoshi, B.E. Rittmann, Microbial ecology of a perchlorate-reducing, hydrogen-based membrane biofilm reactor, Water Res. 42 (2008) 1151–1159.
[16] J. Chung, R. Nerenberg, B.E. Rittmann, Bioreduction of selenate using a hydrogen-based membrane biofilm reactor, Environ. Sci. Technol. 40 (2006) 1664–1671.
[17] J. Chung, R. Nerenberg, B.E. Rittmann, Bio-reduction of soluble chromate using a hydrogen-based membrane biofilm reactor, Water Res. 40 (2006) 1634–1642.
[18] J. Chung, R. Krajmalnik-Brown, B.E. Rittmann, Bioreduction of trichloroethene using a hydrogen-based membrane biofilm reactor, Environ. Sci. Technol. 42 (2008) 477–483.
[19] D.L. Correll, The role of phosphorus in the eutrophication of receiving waters: a review, J. Environ. Qual. 27 (1998) 261–266.
[20] J. Roelofs, Impact of acidification and eutrophication on macrophyte communities in soft waters in The Netherlands I. Field observations, Aquat. Bot. 17 (1983) 139–155.
[21] T. Toolan, J.D. Wehr, S. Findlay, Inorganic phosphorus stimulation of bacterioplankton production in a meso-eutrophic lake, Appl. Environ. Microbiol. 57 (1991) 2074–2078.
[22] J. Li, L.-P. Zhu, Y.-Y. Xu, B.-K. Zhu, Oxygen transfer characteristics of hydrophilic treated polypropylene hollow fiber membranes for bubbleless aeration, J. Membr. Sci. 362 (2010) 47–57.
[23] Y. Tang, C. Zhou, M. Ziv-El, B.E. Rittmann, A pH-control model for heterotrophic and hydrogen-based autotrophic denitrification, Water Res. 45 (2011) 232–240.
[24] J.J. Hudson, W.D. Taylor, D.W. Schindler, Phosphate concentrations in lakes, Nature 406 (2000) 54–56.
[25] S. Xia, C. Wang, X. Xu, Y. Tang, Z. Wang, Z. Gu, Y. Zhou, Bioreduction of nitrate in a hydrogen-based membrane biofilm reactor using CO_2 for pH control and as carbon source, Chem. Eng. J. 276 (2015) 59–64.
[26] S. Xia, Z. Zhang, F. Zhong, J. Zhang, High efficiency removal of 2-chlorophenol from drinking water by a hydrogen-based polyvinyl chloride membrane biofilm reactor, J. Hazard. Mater. 186 (2011) 1367–1373.
[27] S. Xia, H. Li, Z. Zhang, Y. Zhang, X. Yang, R. Jia, K. Xie, X. Xu, Bioreduction of para-chloronitrobenzene in drinking water using a continuous stirred hydrogen-based hollow fiber membrane biofilm reactor, J. Hazard. Mater. 192 (2011) 593–598.
[28] A.V. Bankar, A.R. Kumar, S.S. Zinjarde, Removal of chromium (VI) ions from aqueous solution by adsorption onto two marine isolates of *Yarrowia lipolytica*, J. Hazard. Mater. 170 (2009) 487–494.
[29] S. Xia, J. Li, R. Wang, Nitrogen removal performance and microbial community structure dynamics response to carbon nitrogen ratio in a compact suspended carrier biofilm reactor, Ecol. Eng. 32 (2008) 256–262.
[30] S. Xia, J. Li, S. He, K. Xie, X. Wang, Y. Zhang, L. Duan, Z. Zhang, The effect of organic loading on bacterial community composition of membrane biofilms in a submerged polyvinyl chloride membrane bioreactor, Bioresour. Technol. 101 (2010) 6601–6609.
[31] L. Duan, I. Moreno-Andrade, C.L. Huang, S. Xia, S.W. Hermanowicz, Effects of short solids retention time on microbial community in a membrane bioreactor, Bioresour. Technol. 100 (2009) 3489–3496.
[32] D. Richardson, L. Blom, E. Taylor, The effect of pH on membrane performance in treatment of paper industry effluent, in: 63rd Appita Annual Conference and Exhibition, Melbourne 19–22 April 2009, Appita Inc.,, 2009, p. 249.